Available online at www.sciencedirect.com

ScienceDirect

IFAC PapersOnline CONFERENCE PAPER ARCHIVE

IFAC PapersOnLine 53-2 (2020) 12295–12300

Switching sequences for non-predictive declutching control of wave energy converters

Paula B. Garcia-Rosa *,** **Olav B. Fosso** ** **Marta Molinas** ***

* *SINTEF Energy Research, 7465 Trondheim, Norway (e-mail: paula.garcia-rosa@sintef.no).*

** *Department of Electric Power Engineering, Norwegian University of Science and Technology, NO-7491 Trondheim, Norway (e-mail: olav.fosso@ntnu.no).*

*** *Department of Engineering Cybernetics, Norwegian University of Science and Technology, NO-7491 Trondheim, Norway (e-mail: marta.molinas@ntnu.no)*

Abstract: Aiming at improving the energy absorption from waves, a number of studies have considered declutching control – a phase-control method that consists of disengaging the power take-off (PTO) system from the oscillating body at specific intervals of time. The on/off sequences with the instants to engage/disengage the PTO are usually determined by optimization procedures that require the knowledge of future excitation force, which remains an open challenge for practical implementation. This paper presents a comprehensive numerical study with different PTO damping coefficients for declutching control. It is shown that the value of the damping plays an important role on the efficacy of the control method and on the optimal time to engage (or disengage) the PTO. Then, two switching sequences that use current information of the body motion are proposed, and compared with the threshold unlatching strategy. When the body velocity vanishes, the PTO is clutched (declutched) if the current estimation of the mean excitation force frequency is lower (higher) than the body resonant frequency. The instant to declutch (clutch) again depends on the damping coefficient. The resultant PTO force profiles are not optimal, but act in an effective way to improve the energy absorption, while not requiring wave short-term predictions and numerical optimization solutions that can be time-consuming depending on the fidelity of numerical models and the prediction horizon. Numerical simulations consider real ocean waves and synthetic waves.

Keywords: Renewable energy systems, wave energy, declutching control, on-off actions, numerical simulation.

1. INTRODUCTION

In order to absorb maximum power from waves, control systems require wave forecasting and bi-directional power take-off (PTO) systems. In this framework, control schemes based on model-predictive control are widely studied in the literature, see, e.g., Faedo et al. (2017) for a review. Alternatively, passive control methods are sub-optimal solutions that avoid the need for the PTO to supply power (and hence are named *passive*) while still increasing the absorption when compared to passive loading (PL). In contrast to PL, where the PTO damping is constant, passive control methods can modify the damping on a timely basis, either by tuning it to the frequency of waves (Garcia-Rosa et al., 2019) or by solving an optimization problem to determine the optimal damping profile, which results in on/off sequences (Tom and Yeung, 2013) – a characteristic of the declutching control (DLC) method.

Declutching is a phase-control method that consists of disengaging the PTO system from the oscillating body during some parts of the body motion cycle. The principle is to engage and disengage the PTO in order to allow the oscillating body to "catch up" to the excitation force, and then, bring the body velocity into phase with the excitation force.

The switching sequences for DLC are usually determined by optimization procedures that require the knowledge of future excitation force (Babarit et al., 2009; Teillant et al., 2010; Clément and Babarit, 2012), which remains an open challenge for practical implementation. Babarit et al. (2009) have used an optimization procedure based on Pontryagin principle to determine the instants the PTO system is either on or off. It is shown that changes in the controller state, from off to on, are followed by zero-crossings of the velocity, but a heuristic criterion regarding the instants to switch back the controller state to off has not been identified.

Furthermore, aiming at determining the best damping profile in terms of energy absorption for regular waves, Teillant et al. (2010) have used a general parametrization of the damping force that allowed for two phase-control

10.1016/j.ifacol.2020.12.1172

methods: latching and declutching. While latching locks the body motion for specific intervals of time, declucthing control modifies the body dynamics without locking it. Teillant et al. (2010) have shown that declutching (latching) control is optimal when the wave frequency is higher (lower) than the body resonant frequency. For declutching, the damping changes from upper to lower boundary values when the body velocity vanishes. The duration of time for lower damping, as well as the upper and lower values, were determined through an optimization process with a genetic algorithm and the Nelder-Mead algorithm.

In (Feng and Kerrigan, 2013), the PTO is clutched when the body velocity is zero, and a derivative-free optimization algorithm that reduces the number of function evaluations is proposed to determine for how long the PTO should be active. A comparison of the wave energy converter (WEC) performance for optimization formulations based on past and future wave data is also presented.

To avoid the prediction of future waves, a few studies on declutching have used the *threshold unlatching* strategy (Hals et al., 2011; Garcia-Rosa and Ringwood, 2016). As suggested by the name, the strategy was initially proposed for latching control. It consists of unlatching the body at the instant when the excitation force (or other reference variable) passes a chosen threshold (Lopes et al., 2009).

The aim of this paper is twofold. Firstly, to investigate how the PTO damping coefficient affects the optimal declutching/clutching duration and the efficacy of the control strategy in terms of improving the power absorption in regular wave regimes. Rather than optimizing the PTO damping, the purpose is to identify for which values of damping, declutching control will not represent an efficient solution to improve the energy absorption, when compared to a simpler strategy as passive loading. Then, the goal is to propose switching sequences that do not require estimation of future incident waves. Two strategies that use current information of the body motion are proposed, and compared with the threshold unlatching strategy. Furthermore, in all switching sequences, the decision about clutching (declutching), i.e. engaging (disengaging) the PTO, depends on the current estimation of the dominant frequency of the wave excitation force and on the body resonant frequency. The sequences differ on defining the *instants* to declutch (clutch) again the PTO.

2. DYNAMIC MODELING OF THE WEC

2.1 Equation of Motion

This study considers a single oscillating body represented as a truncated vertical cylinder constrained to move in heave. With the assumption of linear hydrodynamic theory, and neglecting friction and viscous forces, the body motion is described by the superposition of the wave excitation force (f_e), radiation and restoring forces, and the force produced by the PTO mechanism (f_p):

$$M\ddot{x}(t)+\int_0^t h_r(t-\tau)\,\dot{x}(\tau)\,d\tau+Sx(t)=f_e(t)+f_p(t)\,, \quad (1)$$

where $x \in \mathbb{R}$ is the vertical position of the body, $M = [m + m_r(\infty)]$, $m \in \mathbb{R}_+$ is the body mass, $m_r(\infty) \in \mathbb{R}_+$ is the infinite-frequency added mass coefficient, defined with the asymptotic values of the added masses at infinite frequency, $S \in \mathbb{R}_+$ is the buoyancy stiffness, and the kernel of the convolution term $h_r(t-\tau)$ is known as fluid memory term (Cummins, 1962),

$$h_r(t) = \frac{2}{\pi}\int_0^\infty B_r(\omega)\cos(\omega t-\tau)\,d\omega\,, \quad (2)$$

where $B_r(\omega) \in \mathbb{R}_+$ is the radiation damping coefficient, and $\omega \in \mathbb{R}_+$ is the wave frequency.

The excitation force, i.e., the force due to the incident waves is given by

$$f_e(t) = \int_{-\infty}^\infty h_e(t-\tau)\,\zeta(\tau)\,d\tau\,, \quad (3)$$

where h_e is the inverse Fourier transform of the excitation force transfer function $H_e(\omega)$, which has low-pass filter characteristics for floating WECs, and ζ is the wave elevation. Notice that (3) is non-causal, since in fact, the pressure distribution is the cause of the force and not the incident waves (Falnes, 2002).

The mean absorbed power over a time range T is

$$P_a = -\frac{1}{T}\int_0^T f_p(t)\,\dot{x}(t)\,dt\,, \quad (4)$$

where $\dot{x}(t)$ is the velocity of the body. By considering a generic PTO system and PL, the PTO force is defined as

$$f_p(t) = -B_c\,\dot{x}(t)\,, \quad (5)$$

where $B_c \in \mathbb{R}_+$ is the PTO damping.

2.2 Steady-state Sinusoidal Motion

Under passive loading (5), the steady-state response of the body velocity to $f_e(t) = F_e(\omega)\cos\omega t$ is given by $\dot{x}_{ss}(t) = |H(j\omega)|F_e(\omega)\cos(\omega t + \phi(\omega))$, where

$$H(j\omega) = \frac{1}{(B_c + B_r(\omega)) + j(\omega(m + m_r(\omega)) - S/\omega)}\,, \quad (6)$$

$$\phi(\omega) = -\arctan\left[\frac{\omega(m + m_r(\omega)) - S/\omega}{B_c + B_r(\omega)}\right]\,, \quad (7)$$

and $F_e(\omega) \in \mathbb{R}_+$ is the excitation force coefficient. By assuming the body resonant frequency is $\omega_r \approx \sqrt{S/(m+m_r(\omega))}$, the phase (7) between the velocity and the excitation force can be rewritten as

$$\phi(\omega) = -\arctan\left[\frac{(m + m_r(\omega))(\omega^2 - \omega_r^2)}{\omega(B_c + B_r(\omega))}\right]\,. \quad (8)$$

From (8), it can be noted that when

- $\omega < \omega_r$, then $\phi(\omega) > 0$, and the velocity leads the excitation force;
- $\omega > \omega_r$, then $\phi(\omega) < 0$, and the velocity lags the excitation force;
- $\omega = \omega_r$, then $\phi(\omega) = 0$, and the velocity is in phase with the excitation force.

Furthermore, for regular wave regime and PL, the optimal constant damping and the average power absorbed by the WEC are, respectively, calculated as (Falnes, 2002):

$$B_{c,opt}(\omega) = \sqrt{(B_r(\omega))^2 + (\omega(m + m_r(\omega)) - S/\omega)^2}\,, \quad (9)$$

$$P_{c,opt} = \frac{B_{c,opt}(\omega) F_e(\omega)^2}{2(B_{c,opt}(\omega) + B_r(\omega))^2}\,. \quad (10)$$

3. SWITCHING SEQUENCES FOR DECLUTCHING CONTROL

Here we assume a generic PTO system, where the PTO force is expressed as

$$f_p(t) = -B_p\, \dot{x}(t) u(t)\,, \quad (11)$$

$B_p \in \mathbb{R}_+$ is the PTO damping, and the control signal $u(t)$ has two states: on ($u=1$) or off ($u=0$).

As discussed in Section 2.2, when the incident wave frequency is lower than the body resonant frequency, the velocity is leading the excitation force by a certain phase shift. Then, the phase-control method should act to slow down the natural response of the body in order to force the velocity to be in phase with the excitation force. Conversely, the controller should act to speed up the natural response of the body when the wave frequency is higher than the WEC resonant frequency.

Following previous studies (Teillant et al., 2010), the PTO force profile is determined according to the incident wave frequency and the resonant frequency of the oscillating body. However, only the clutching concept, i.e. engage/disengage the PTO, is applied here. Thus, for

- $\omega < \omega_r$: To slow down the device motion, the PTO is connected, i.e. clutched ($u = 1$), when the body velocity vanishes, and disconnected, i.e. declutched ($u=0$), in a certain instant of time to be determined.
- $\omega > \omega_r$: To allow the device to move "faster", the PTO is disconnected ($u=0$) when the body velocity vanishes, and connected ($u=1$) in a certain instant of time to be determined.

The objective is to propose causal control laws for DLC by performing a comprehensive numerical study using regular waves at first. Using different values of damping, optimal clutching durations are determined for the cases when $\omega < \omega_r$, and optimal declutching durations, for the cases when $\omega > \omega_r$. In such a way, the effect of the PTO damping on the control strategy is also investigated. In what follows, numerical simulations are performed considering the same heaving cylinder adopted in (Garcia-Rosa et al., 2017). The cylinder has a radius of 5 m, draught of 4 m, mass $m = 3 \times 10^5$ kg and resonant frequency $\omega_r = 1.2$ rad/s.

3.1 Optimal clutching/declutching duration

The optimal clutching/declutching duration in seconds ($\Delta t_{h,opt}$) that optimizes the power absorbed by the WEC with decltuching control is determined via simulations with a complete set of possible values for the time interval. Figure 1 (right) illustrates the optimal intervals of time obtained for different PTO coefficients and regular waves with amplitude of 1 m and some specific frequencies. The PTO damping coefficients are defined as

$$B_p = \bar{B}_p B_{c,opt}(\omega)\,, \quad (12)$$

for each wave frequency ω, where $\bar{B}_p$ is a dimensionless constant, $0.5 \leq \bar{B}_p \leq 20$, and $B_{c,opt}(\omega)$ is the optimal

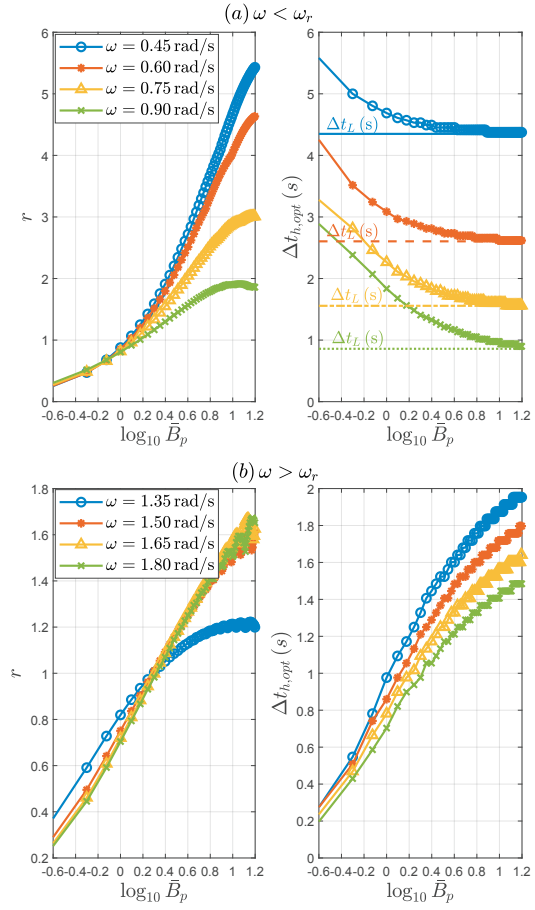

Fig. 1. Evolution of optimal time (right) and ratio of power (left) versus PTO damping in regular waves. (a) Optimal clutching duration, $\omega < \omega_r$; (b) Optimal declutching duration, $\omega > \omega_r$. The lines in (a) represent the latching duration for each one of the frequencies.

constant damping (9). It can be noted that, for $\omega < \omega_r$, as the value of the damping increases, the optimal clutching duration reduces and tends to the latching duration. The latching duration, denoted as Δt_L in Fig. 1.a (right), is calculated as half the difference between the wave period and the body resonant period (Babarit and Clément, 2006). When the damping is too high ($20 B_{c,opt}(\omega)$) and $u=1$, the PTO force (11) restricts the motion of the body, and consequently, declutching control acts in a similar way as latching control for the cases when $\omega < \omega_r$. Conversely, when $\omega > \omega_r$ the optimal declutching duration increases with the damping.

The ratio of power, calculated as $r = P_a / P_{c,opt}$, is also shown in Figure 1 (left). For $\omega < \omega_r$ and $B_p < 2 B_{c,opt}(\omega)$, DLC will result in less power absorption than the optimal PL power, $P_{c,opt}$ (10), or about the same value. Thus, the value of damping is also important for the efficacy of the strategy. This is further evidenced by Figure 2, which shows the evolution of the ratio of power for different wave frequencies, PTO damping coefficients, optimal clutching duration (Fig. 2.a) and optimal declutching duration (Fig. 2.b). For $\omega > \omega_r$ and the WEC considered in this study, the damping for the declutching strategy should be higher than $2 B_{c,opt}(\omega)$ to allow an energy absorption greater than optimal passive loading.

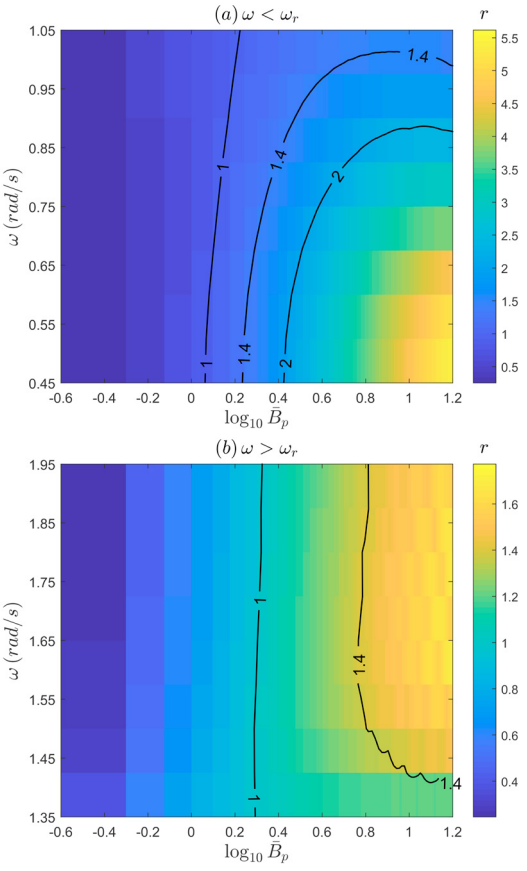

Fig. 2. Ratio of power as a function of PTO damping and wave frequencies in regular waves with (a) optimal clutching duration (b) optimal declutching duration.

To illustrate how the behaviour of system variables changes according to PTO damping for $\omega < \omega_r$, Figure 3 shows the time-series of normalized variables ($\bar{f}_e, \bar{x}, \dot{\bar{x}}, \overline{x\dot{x}}$) and the control signal (u). Constants $\bar{B}_p = 1.5$ (Fig 3.a), and $\bar{B}_p = 5$ (Fig. 3.b), are used with their corresponding optimal clutching duration. The instants u change from on to off occur very close to the instants the position is zero, or equivalently, when the signal $x\dot{x}$ has a positive zero crossing. Nonetheless, the same conclusion cannot be drawn when $\bar{B}_p = 5$ (Fig. 3.b). In such a case, the high damping force employed after the velocity zero crossing causes the velocity to remain around zero, almost stopping the body motion, and thus, neither x nor $x\dot{x}$ provide a good indication for disengaging the PTO.

For $\omega > \omega_r$, the instants when $\dot{x} = 0$ define the instants to disengage the PTO. Figure 4 illustrates the time-series of normalized variables and the control signal when $\bar{B}_p = 2.5$ (Fig 4.a), and $\bar{B}_p = 5$ (Fig. 4.b), with their corresponding optimal declutching duration. It is noted that the intervals while $u = 1$ coincide with intervals the body is speeding up, i.e. acceleration and velocity are in the same direction, and the optimal instant the PTO is switched on occurs when the device starts to slow down (Fig. 4.a), i.e. $\dot{x}\ddot{x} < 0$, or a few seconds after it (Fig. 4.b) depending on the damping.

3.2 Switching sequences without prediction of future waves

This section proposes two strategies to determine the instants the control signal u is either on or off, based on the

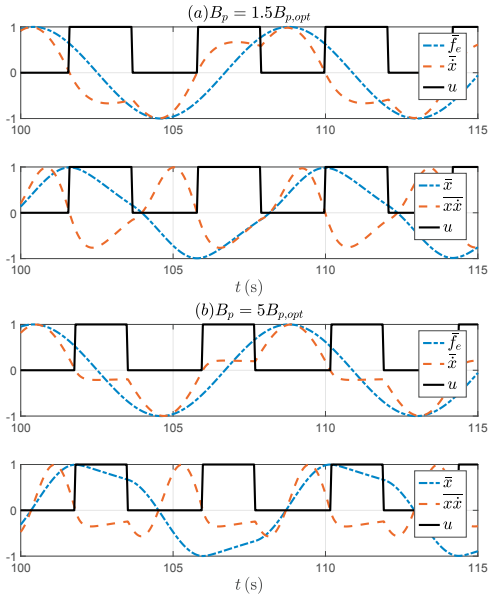

Fig. 3. Time-series of normalized variables and control signal for (a) $B_p = 1.5B_{c,opt}$, and (b) $B_p = 5B_{c,opt}$. ($\omega = 0.75$ rad/s, optimal clutching duration).

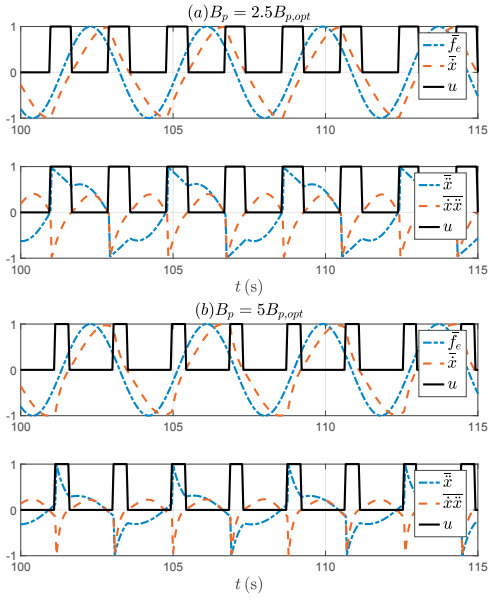

Fig. 4. Time-series of normalized variables and control signal for (a) $B_p = 2.5B_{c,opt}$, and (b) $B_p = 5B_{c,opt}$. ($\omega = 1.65$ rad/s, optimal declutching duration).

observations from Section 3.1. The strategies are evaluated through a comparison with the unlatching threshold strategy, when the WEC is submitted to synthetic irregular waves and real ocean waves. Since such waves are not defined by a single frequency, and the oscillating body has low-pass filter characteristics, the mean centroid frequency of the excitation force (ω_{1,f_e}) is adopted in replacement to the wave frequency ω of regular wave cases.

The mean centroid frequency of the excitation force can be estimated, e.g., by the extended Kalman filter (EKF) as shown in (Garcia-Rosa et al., 2019). In such a case, $f_e(t)$ has to be estimated as well. Note that the switching sequences proposed here rely only on the estimation of the

frequency. Thus, an alternative scheme using real wave measurements and $H_e(\omega)$ could be adopted to obtain an estimation of the mean frequency of the excitation force.

The following switching sequences, denoted respectively as D1 and ¬D2, are proposed for the cases when $\omega_{1,f_e} < \omega_r$:

$$u(t) = \begin{cases} 1\,, & x\dot{x}(t) \leq 0\,, \\ 0\,, & x\dot{x}(t) > 0\,, \end{cases} \tag{13}$$

and for the cases when $\omega_{1,f_e} > \omega_r$:

$$u(t) = \begin{cases} 0\,, & \dot{x}\ddot{x}(t) \geq 0\,, \\ 1\,, & \dot{x}\ddot{x}(t) < 0\,. \end{cases} \tag{14}$$

For threshold unlatching strategies, denoted here as D3 and D4, $\dot{x}=0$ triggers the control state until $f_e(t)$ passes a chosen threshold (Lopes et al., 2009). Table 1 summarizes the switching sequences, where D1–D4 are applied when $\omega_{1,f_e} < \omega_r$, ¬D1–¬D4 are applied when $\omega_{1,f_e} > \omega_r$. The symbol ¬ represents logical negation.

Three wave elevation records off the west coast of Ireland (as in Garcia-Rosa et al. (2019)), referred as sea states S1–S3, and six irregular waves (Ir1–Ir6) are adopted as inputs to the WEC. For each real sea state, two irregular waves are generated by modifying the parameters of Ochi spectral distributions (Ochi, 1998). Figure 5 illustrates the wave spectra of sea states and synthetic waves (top), and the corresponding excitation force spectra (bottom). The significant wave height H_s of the wave spectra, and the mean centroid frequency for both the wave (ω_1) and the excitation force spectra (ω_{1,f_e}) are shown in Table 2.

The simulation interval is about 30 min for each case. A comparison in terms of power absorption for the switching sequences (Table 1) with PL power is shown in Figure 6. The ratio r_c is calculated as P_a/P_c, where P_a is the power absorbed by the WEC when DLC is applied, and P_c is the PL power with damping tuned at frequency ω_{1,f_e}. As suggested by the analysis of Fig. 3, D1 results in the greatest energy absorption when the damping is around 1.5 to $2.5B_c(\omega_{1,f_e})$ for waves Ir1–Ir3 and Ir5. Such waves have mean centroid frequencies much lower than the body resonant frequency (1.2 rad/s). As the damping increases, the best strategies become the threshold unlatching (D3, D4). Such strategies do not rely on the dynamic motion of the WEC to switch off the control signal. Furthermore, the benefit of applying DLC using D1–D4 in Ir4 is lower than the other cases, since ω_{1,f_e} is very close to ω_r. Finally, when $\omega_{1,f_e} > \omega_r$ (Ir6) and $B_p < 4B_c(\omega_{1,f_e})$, sequence ¬D2 is the best choice. ¬D2 defines the time interval in which the WEC is speeding up (slowing down) as the time interval the control signal is off (on), and thus, it allows the body to gain momentum.

In order to compare the strategies with best performances in terms of power absorption for $\omega_{1,f_e} < \omega_r$, Table 3 summarizes the obtained results for S1–S3 with D1 ($\bar{B}_p = 2$) and D4 ($\bar{B}_p = 5$). A comparison of the peak-to-average power ratio (PTO rating), maximum PTO force, and maximum displacement of the body are included with the ratio r_c. Although the strategy D4 with $\bar{B}_p = 5$ results in the greatest power in most of the cases, it requires higher PTO forces and larger displacements of the body than D1. It is important to note that constraints on the PTO force and body motion are not considered here, but for practical

Table 1. Switching sequences

	Condition	$u(t)$	Str.	Condition	$u(t)$
D1	$x\dot{x} \leq 0$ $x\dot{x} > 0$	1 0	¬D1	$x\dot{x} \leq 0$ $x\dot{x} > 0$	0 1
D2	$\dot{x}\ddot{x} \geq 0$ $\dot{x}\ddot{x} < 0$	1 0	¬D2	$\dot{x}\ddot{x} \geq 0$ $\dot{x}\ddot{x} < 0$	0 1
D3	trigger: $\dot{x}=0$ thres: $\dot{f}_e=0$	1 0	¬D3	trigger: $\dot{x}=0$ thres: $\dot{f}_e=0$	0 1
D4	trigger: $\dot{x}=0$ thres: $f_e=0$	1 0	¬D4	trigger: $\dot{x}=0$ thres: $f_e=0$	0 1

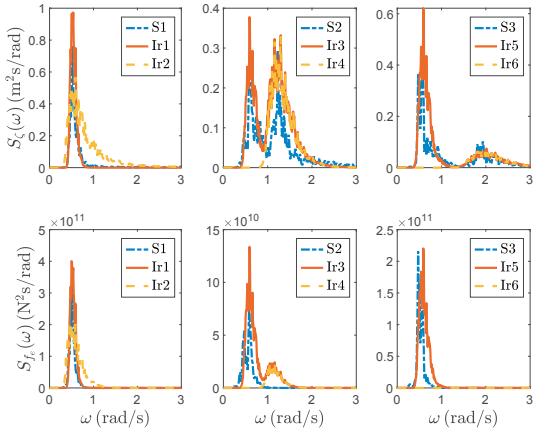

Fig. 5. Wave spectra of real data and synthetic irregular waves (top), and excitation force spectra (bottom).

Table 2. Significant wave height H_s (m), wave mean centroid frequency ω_1 (rad/s), and excitation force mean centroid frequency ω_{1,f_e} (rad/s) for S1–S3 and Ir1–Ir6.

	S1	Ir1	Ir2	S2	Ir3	Ir4	S3	Ir5	Ir6
H_s	1.26	1.50	2.00	1.43	1.85	1.49	1.39	1.67	0.90
ω_1	0.70	0.54	0.91	1.18	1.12	1.37	1.18	1.09	2.18
ω_{1,f_e}	0.55	0.54	0.61	0.73	0.75	1.18	0.59	0.61	1.74

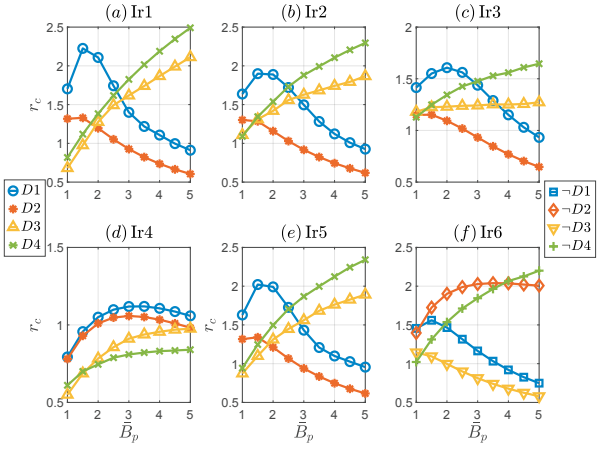

Fig. 6. Ratio r_c for irregular waves (Ir1-Ir6).

application studies, the physical limits of both the body excursion and PTO have to be taken into account. Figure 7 shows a sample of time-series simulation for S1 with D1 ($\bar{B}_p = 2$) when the excitation force frequency is estimated by the extended Kalman filter.

Table 3. Ratio r_c, PTO rating, maximum PTO force, and maximum body displacement for D1 and D4 in S1–S3.

Sea	Strategy	r_c	P_{max}/P_a	$f_{p,max}$ (kN)	x_{max} (m)
S1	D1 ($\bar{B}_p=2$)	2.07	8.93	750.5	1.13
	D4 ($\bar{B}_p=5$)	2.47	8.84	1.29×10^3	2.27
S2	D1 ($\bar{B}_p=2$)	1.69	14.12	624.5	1.03
	D4 ($\bar{B}_p=5$)	1.68	15.02	1.02×10^3	1.64
S3	D1 ($\bar{B}_p=2$)	2.02	13.73	808.1	1.33
	D4 ($\bar{B}_p=5$)	2.16	12.33	1.25×10^3	2.16

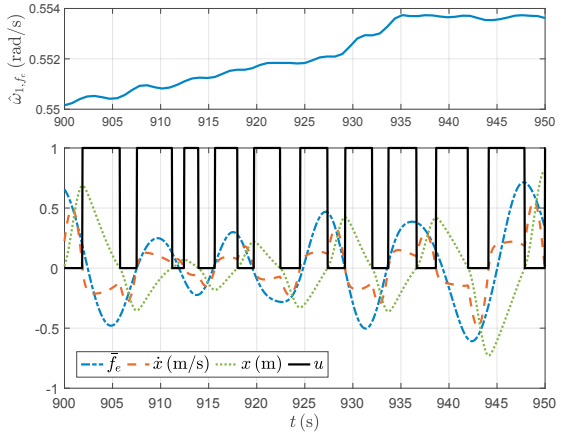

Fig. 7. Time-series of EKF estimated frequency (top), normalized excitation force, velocity, position, and control signal for S1 with D1 and $\bar{B}_p=2$ (bottom).

4. CONCLUSIONS

A comprehensive numerical study with different PTO damping coefficients showed that the value of damping plays an important role on the efficacy of the declutching control method and also on the optimal time to engage (or disengage) the PTO. Thus, the switching sequences for non-predictive control should take into account the value of the damping, or the PTO force applied.

Furthermore, the switching sequences proposed here rely on current estimations of the mean centroid frequency of the excitation force and on the body resonant frequency. The decision about clutching (declutching) the WEC, i.e. engaging (disengaging) the PTO, is defined according to current estimations only. When the body velocity vanishes, the PTO is clutched (declutched) if the estimated mean frequency is lower (higher) than the body resonant frequency. The switching sequences differ on defining the *instants* to declutch (clutch) the PTO again.

For a generic PTO system, the results showed that when the declutching damping is twice PL damping as defined by (9), the variables of motion (position, velocity, acceleration) can be used for defining both the instants to clutch and declutch. For instance, when the mean excitation force frequency is higher than the body resonant frequency, the PTO is disengaged while the body is speeding up (i.e. velocity and acceleration are in the same direction $\dot{x}\ddot{x}(t) \geq 0$) to allow the body to gain momentum, and engaged while the body is slowing down (i.e. $\dot{x}\ddot{x}(t) < 0$).

However, the switching sequences relying on the motion to define both instants to clutch and declutch are only meaningful if the body motion is not excessively restricted by high damping forces during clutching (e.g., when the damping is five times the passive loading damping). In such cases, the threshold unlatching strategy is the best option for defining the switching sequences if wave forecasting is to be avoided.

REFERENCES

Babarit, A. and Clément, A.H. (2006). Optimal latching control of a wave energy device in regular and irregular waves. *Applied Ocean Research*, 28(2), 77–91.

Babarit, A., Guglielmi, M., and Clément, A. (2009). Declutching control of a wave energy converter. *Ocean Engineering*, 36, 1015–1024.

Clément, A.H. and Babarit, A. (2012). Discrete control of resonant wave energy devices. *Philos. Trans. Roy. Soc. A, Math. Phys. Eng. Sci.*, 370(1959), 288–314.

Cummins, W.E. (1962). The impulse response function and ship motions. *Schiffstechnik*, 47(9), 101–109.

Faedo, N., Olaya, S., and Ringwood, J.V. (2017). Optimal control, MPC and MPC-like algorithms for wave energy systems: An overview. *IFAC Journal of Systems and Control*, 1, 37–56.

Falnes, J. (2002). *Ocean Waves and Oscillating Systems: Linear Interaction including Wave-Energy Extraction.* Cambridge Univ. Press, USA.

Feng, Z. and Kerrigan, E.C. (2013). Latching control of wave energy converters using derivative-free optimization. In *Proc. of the IEEE 52nd Annual Conf. on Decision and Control*, 7474–7479. Florence, Italy.

Garcia-Rosa, P.B., Kulia, G., Ringwood, J.V., and Molinas, M. (2017). Real-time passive control of wave energy converters using the Hilbert-Huang transform. In *IFAC-PapersOnLine 50-1*, (Proc. of the 20th IFAC World Congress), 14705–14710. Toulouse, France.

Garcia-Rosa, P.B. and Ringwood, J.V. (2016). On the sensitivity of optimal wave energy device geometry to the energy maximising control system. *IEEE Trans. Sustainable Energy*, 7(1), 419–426.

Garcia-Rosa, P.B., Ringwood, J.V., Fosso, O.B., and Molinas, M. (2019). The impact of time–frequency estimation methods on the performance of wave energy converters under passive and reactive control. *IEEE Trans. Sustainable Energy*, 10(4), 1784–1792.

Hals, J., Falnes, J., and Moan, T. (2011). A comparison of selected strategies for adaptive control of wave energy converters. *J. of Offshore Mech. and Arctic Eng.*, 133(3), 031101–031113.

Lopes, M.F.P., Hals, J., Gomes, R.P.F., Moan, T., Gato, L.M.C., and Falcão, A.F.O. (2009). Experimental and numerical investigation of non-predictive phase-control strategies for a point-absorbing wave energy converter. *Ocean Engineering*, 36(5), 386–402.

Ochi, M.K. (1998). *Ocean waves: The stochastic approach.* Cambridge Ocean Technology Series, Cambridge Univ. Press, USA.

Teillant, B., Gilloteaux, J.C., and Ringwood, J.V. (2010). Optimal damping profile for a heaving buoy wave energy converter. In *Proc. of the 8th IFAC Conf. on Control App. in Marine Systems*, 360–365. Rostock, Germany.

Tom, N. and Yeung, R.W. (2013). Nonlinear model predictive control applied to a generic ocean-wave energy extractor. In *Proc. of the 32nd Int. Conf. on Ocean, Offshore and Arctic Eng. (OMAE 2013)*. Nantes, France.